SUPPLEMENTARY INFORMATION

Temperature dependence of the electron and hole Landé g-factors in $CsPbI_3$ nanocrystals in a glass matrix

Sergey R. Meliakov, Evgeny A. Zhukov, Vasilii V. Belykh, Mikhail O. Nestoklon, Elena V. Kolobkova, Maria S. Kuznetsova, Manfred Bayer, Dmitri R. Yakovlev

S1. Photoluminescence and absorption spectra of $CsPbI_3$ NCs

The photoluminescence (PL) spectra are excited by a continuous-wave laser operating at the wavelength of 405 nm (3.06 eV) with a power of 0.5 mW. The absorption spectra are measured using a Cary 6000i UV Vis-NIR spectrophotometer. The spectra measured at the temperature of $T = 6$ K for the three studied samples are presented in Figure S1. The shift to higher energies among the samples results from a decrease of the NC size from sample #1 towards sample #3. The significant width of the PL emission lines and of the exciton absorptions peaks indicates a significant dispersion of the NC sizes in each sample. For all samples, a Stokes shift of the PL maximum from the absorption maximum is observed.

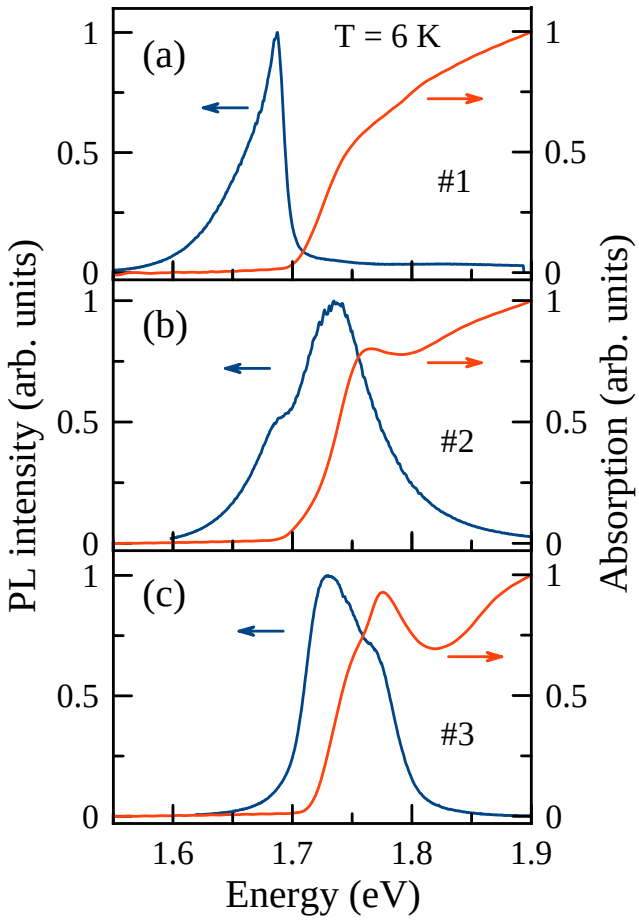

FIG. S1. Normalized photoluminescence (blue line) and absorption (red line) spectra of the studied $CsPbI_3$ NCs: (a) sample #1, (b) sample #2 and (c) sample #3. $T = 6$ K.

Figures S2(a,b,c) show the absorption spectra of the samples under study, measured for temperatures from 4 K up to 150 K. The edge of the absorption for all samples shifts to higher energies with increasing temperature. For samples #2 and #3 the dependence of the shift on temperature, presented in Figures S2(e,f), was evaluated from the shift of the maximum of the exciton absorption peak. For sample #1, the exciton peak is significantly broadened so that its maximum is almost impossible to determine precisely. Therefore, the temperature shift of the absorption

edge was evaluated from the position of the half-maximum in the absorption edge. It should also be noted that for all samples a significant shift was observed only at temperatures above $T \simeq 12$ K. At high T, the shift increases almost linearly with temperature. This is demonstrated by the linear fits of the dependences in Figures S2(d,e,f). The slopes of these lines are: 3.2×10^{-4} eVK^{-1} (#1), 3.8×10^{-4} eVK^{-1} (#2), and 3.5×10^{-4} eVK^{-1} (#3).

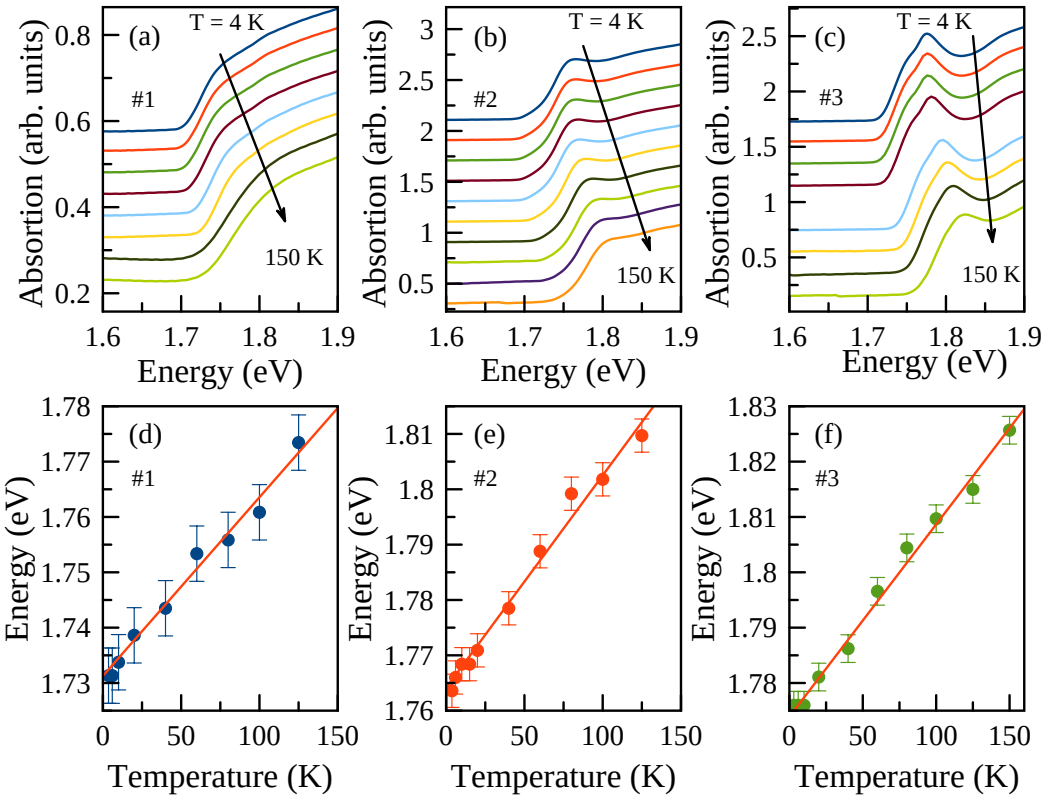

FIG. S2. Absorption spectra of sample #1 (a), #2 (b), and #3 (c) in the temperature range of $T = 4 - 150$ K. (d),(e),(f) Dependences of the shift of the absorption edge on temperature for samples #1, #2 and #3, respectively. Red lines are linear fits to the measured dependences with parameters given in text.

S2. Spin dynamics in different magnetic fields

Figure S3a plots the FE dynamics in sample #1 at $T = 6$ K for the laser photon energy of 1.722 eV. The spot on the sample on which the measurements are carried out differs from the spot corresponding to Figure 1. Here, the hole spin precession is almost invisible. Therefore, it is possible to evaluate only the electron spin parameters. Figure S3b shows the magnetic field dependence of the electron Larmor precession frequency. A fit to these data with eq. (1) gives the electron g-factor $g_e = 2.26$. The magnetic field dependence of the electron spin dephasing time $T^*_{2,e}$ is presented in Figure S3c. $T^*_{2,e}$ decreases with growing magnetic field from about 800 ps at zero field to 200 ps at the maximum magnetic field of 430 mT. Fitting the data with eq. (3) gives the electron g-factor spread $\Delta g_e = 0.17$.

Figure S4 plots similar data for sample #2, measured at $E_L = 1.703$ eV. Here we observe both electron and hole spin precession. The slopes of the Larmor precession frequency dependences on magnetic field give $g_e = 2.29$ and $g_h = -0.13$ (the sign of the hole g-factor is taken according to Figure 1e). The decrease of the electron and hole spin dephasing times with growing magnetic field corresponds to $\Delta g_e = 0.36$ and $\Delta g_h = 0.10$, respectively.

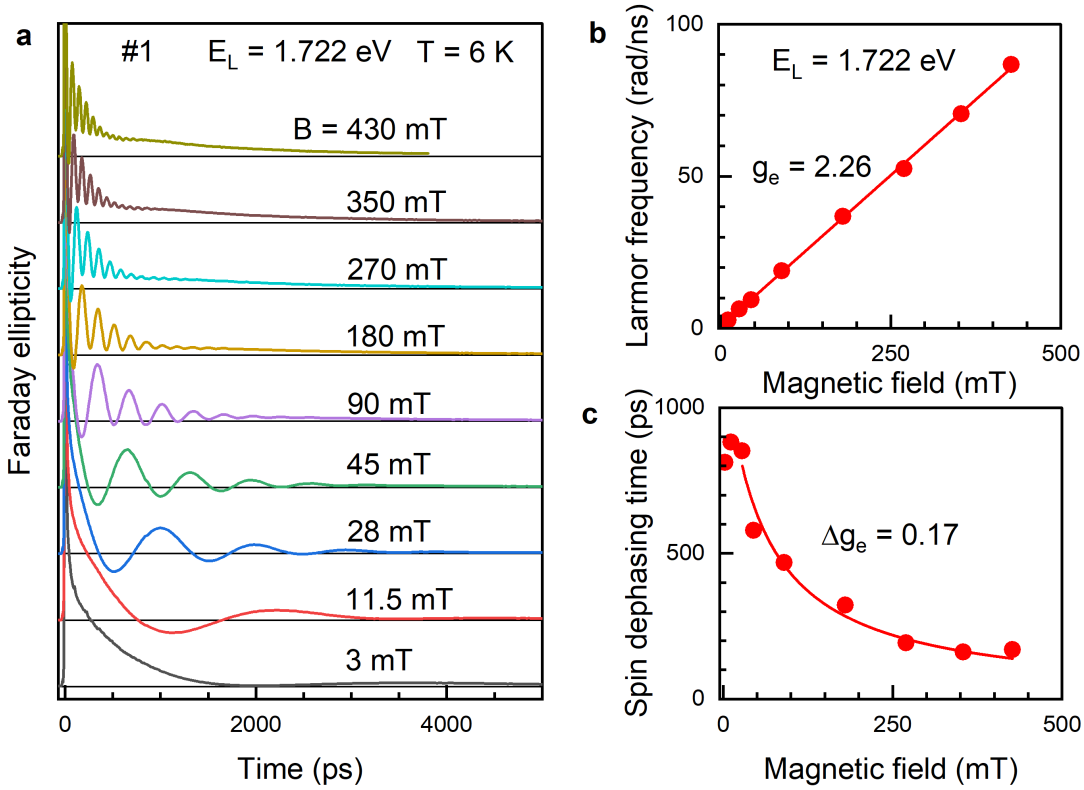

FIG. S3. Magnetic field dependence of spin dynamics at $T = 6$ K for laser photon energy $E_L = 1.722$ eV in sample #1. (a) TRFE dynamics measured in various magnetic fields from 3 mT up to 430 mT. (b) Magnetic field dependence of the electron Larmor precession frequency. Line shows a fit with eq. (1). The slope of the fit corresponds to $g_e = 2.26$. (c) Magnetic field dependence of the electron spin dephasing time. Fitting the experimental data with eq. (3) (line) yields $\Delta g_e = 0.17$.

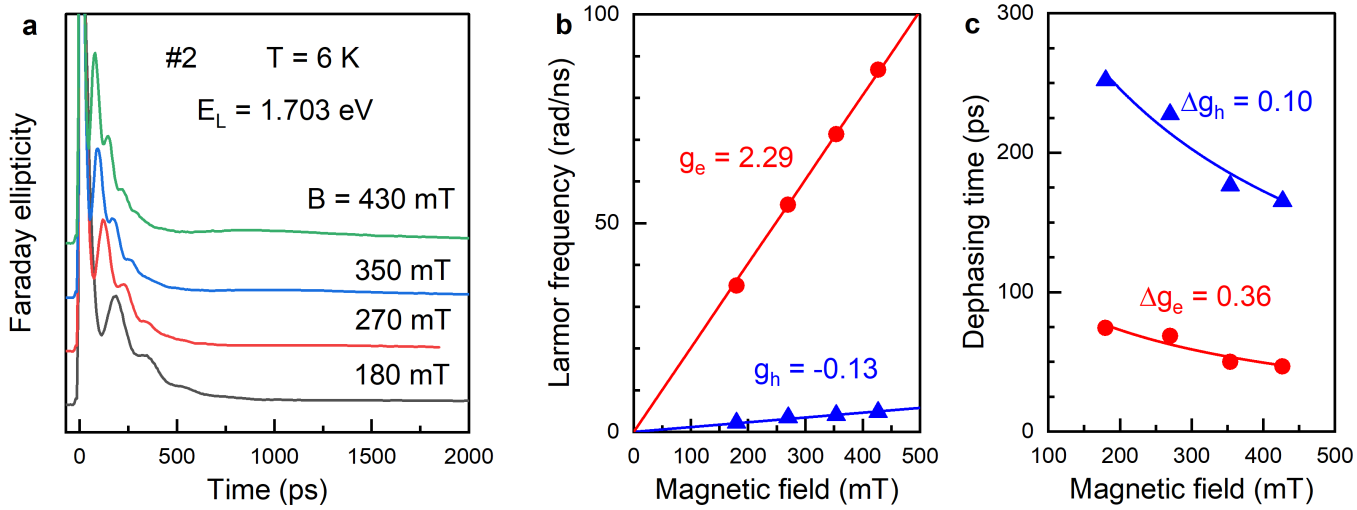

FIG. S4. Magnetic field dependence of the spin dynamics in sample #2 measured at $T = 6$ K for $E_L = 1.703$ eV. (a) FE dynamics measured in various magnetic fields from 180 mT up to 430 mT. (b) Dependences of the hole (blue triangles) and electron (red circles) Larmor precession frequencies on magnetic field. Lines show fits using eq. (1). The slopes of the fits correspond to $g_e = 2.29$ and $g_h = -0.13$. (c) Magnetic field dependences of the electron (red circles) and hole (blue triangles) spin dephasing times. Fits to the experimental data with eq. (3) (lines) yield $\Delta g_e = 0.36$ and $\Delta g_h = 0.10$.

S3. Sign of the hole g-factor

Figure S5 plots the dependence of the absolute value of the hole g-factor on the laser photon energy E_L (the corresponding spectral dependence of g_h is shown in Figure 1e). $|g_h|$ behaves in a nonmonotonic way with growing energy: it decreases in the spectral range from 1.69 eV to 1.71 eV, is close to zero at $E_L \approx 1.71$ eV, and increases in the range from 1.71 eV to 1.78 eV. According to Ref. [Nestoklon, et al., *Nano Lett.* 2023, **23**, 8218] g_h should monotonically change in this spectral range with increasing confinement energy in $CsPbI_3$ NCs, starting from negative values and rising toward positive values. Thus, we suggest that $g_h < 0$ at $E_L < 1.71$ eV, g_h crosses zero at $E_L \approx 1.71$ eV, and $g_h > 0$ at $E_L > 1.71$ eV. We use this hypothesis for presenting data in the main text, e.g., in Figure 1e.

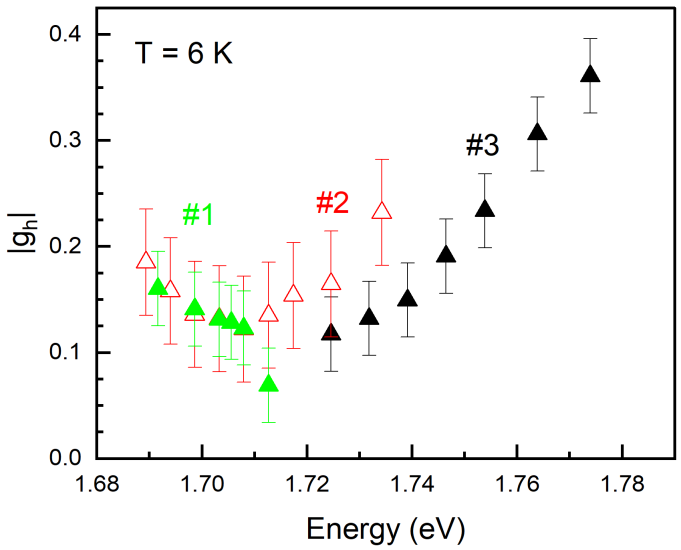

FIG. S5. Spectral dependence of the absolute value of the hole g-factor in samples #1 (green triangles), #2 (red open triangles), and #3 (black triangles). Error bars correspond to the spreads of the g-factor distribution $\Delta g_h \approx 0.07$ for samples #1 and #3 and $\Delta g_h \approx 0.10$ for sample #2.

S4. Spin dynamics at temperatures up to 120 K

Figure S6 shows the temperature dependence of the spin dynamics in sample #1. The Voigt magnetic field is equal to 430 mT. These measurements are performed on a sample spot different from that used for the measurements in Figure 2. The laser energy E_L is adjusted to the maximum of the signal for each temperature. Figure S6a presents the FE dynamics in sample #1 at various temperatures from 9 K to 120 K. We do not observe hole spin oscillations up to temperature of about 50 K. Figures S6b and S6c show the temperature dependences of the electron and hole g-factors. Figure S6d shows corresponding laser photon energies E_L. The g-factor behavior with growing temperature is in agreement with the results presented in the main text.

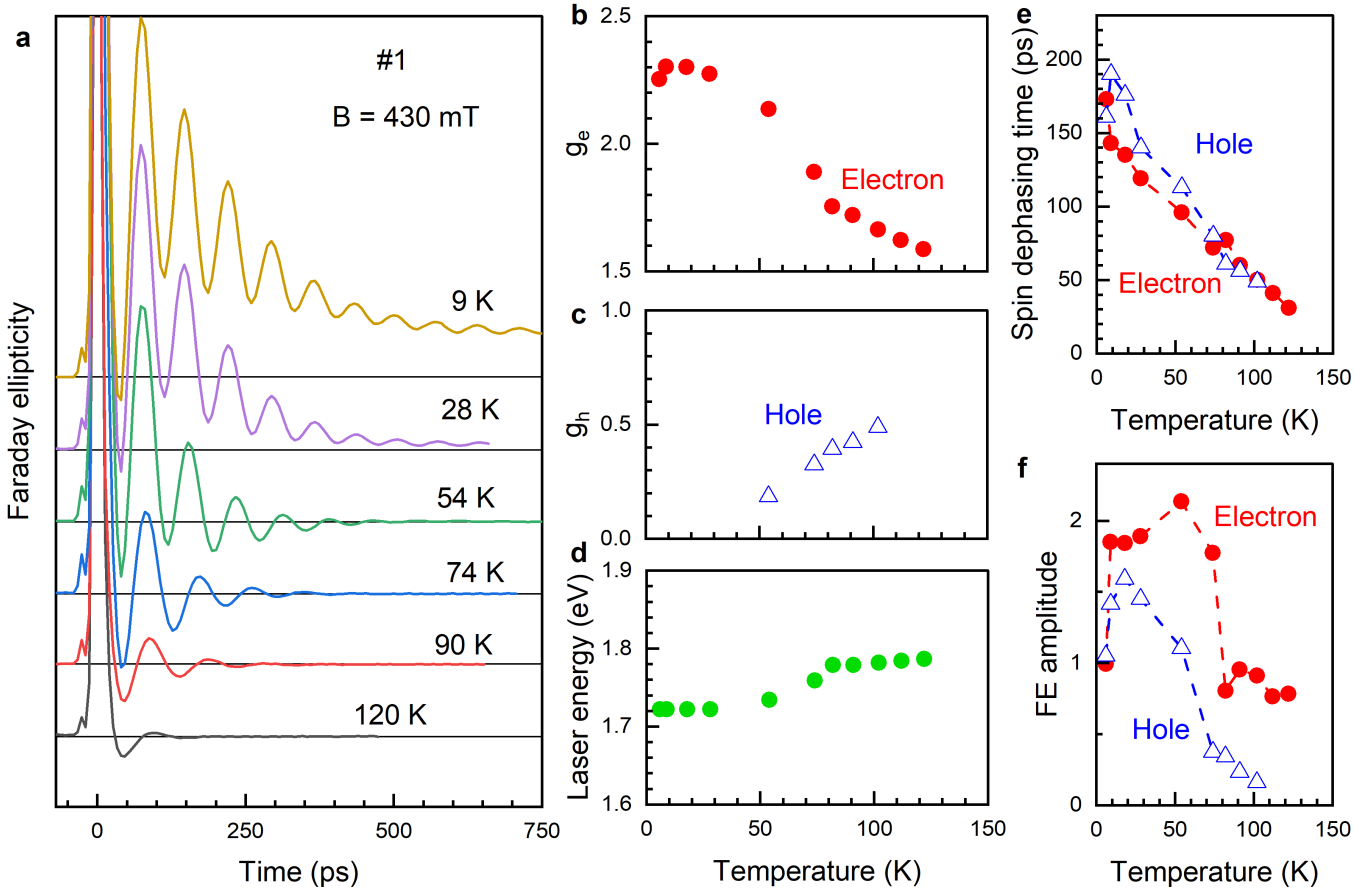

FIG. S6. Temperature dependence of the spin dynamics in sample #1 measured in the Voigt magnetic field of 430 mT. (a) TRFE traces at various temperatures from 9 K to 120 K. They are shifted vertically for clarity. (b,c) Temperature dependences of the electron and hole g-factors. (d) Laser photon energies at which the spin dynamics at various temperatures are measured. (e) Temperature dependence of the spin dephasing times T_2^* for electrons (red circles) and holes (blue triangles). (f) Temperature dependence of the FE amplitudes for electrons (red circles) and holes (blue triangles).

S5. Theory

In this section we estimate the change of the effective band gap, masses, and g-factors in $CsPbI_3$ nanocrystals as function of temperature. We start from the bulk material parameters. In Ref. [39], a linear change of the band gap as function of temperature is observed, with the slope for bulk $CsPbI_3$ given by $\frac{\partial E_g}{\partial T} \approx 3.1 \times 10^{-4}$ eVK^{-1}. For the analysis, it is more convenient to use this value divided by the band gap

$$\xi = \frac{1}{E_g}\frac{\partial E_g}{\partial T} \approx 1.8 \times 10^{-4}\,\mathrm{K}^{-1}\,. \tag{S1}$$

We will also take into account the linear extension of the lattice with temperature

$$\lambda = \frac{1}{a_0}\frac{\partial a_0}{\partial T}\,, \tag{S2}$$

for $CsPbI_3$ $\lambda \approx 3.39 \times 10^{-5}$ K^{-1} [40].

As mentioned in Ref. [39], the change of the band gap leads to renormalization of the effective masses of the charge carriers, which may be estimated assuming that this change is small. In the $\mathbf{k}\cdot\mathbf{p}$ method, the effective masses of the carriers are [27]:

$$\frac{m_0}{m_e} = 1 + \frac{2}{3}\frac{p^2}{m_0 E_g}\,, \tag{S3a}$$

$$\frac{m_0}{m_h} = -1 + \frac{2}{3}\frac{p^2}{m_0 E_g}\frac{3E_g}{E_g+\Delta}\,, \tag{S3b}$$

where Δ is the spin-orbit splitting of the conduction band. Assuming all changes to be small, we may estimate the linear slopes of the mass changes by differentiating Eqs. (S3), giving the result

$$\frac{1}{m_e}\frac{\partial m_e}{\partial T} = \left(1 - \frac{m_e}{m_0}\right)\frac{1}{E_g}\frac{\partial E_g}{\partial T}\,, \tag{S4a}$$

$$\frac{1}{m_h}\frac{\partial m_h}{\partial T} = \left(1 - \frac{m_h}{m_0}\right)\left(1 - \frac{2\Delta}{E_g+\Delta}\right)\frac{1}{E_g}\frac{\partial E_g}{\partial T}\,. \tag{S4b}$$

Using the actual parameters of $CsPbI_3$, where $m_{e,h} \ll m_0$ and $\Delta \approx E_g$, for the estimations it is safe to approximate like

$$\frac{1}{m_e}\frac{\partial m_e}{\partial T} \approx \frac{1}{E_g}\frac{\partial E_g}{\partial T}\,, \quad \frac{1}{m_h}\frac{\partial m_h}{\partial T} \approx 0\,. \tag{S5}$$

Note that in Ref. [39] the authors neglect the contribution to the hole mass from the spin-split electron band and thus severely overestimate its change.

Next, we need to estimate the change of the effective band gap. It may be evaluated as

$$\frac{1}{E_{qc}}\frac{\partial E_{qc}}{\partial T} = -\left[\frac{1}{m_{e,h}}\frac{\partial m_{e,h}}{\partial T} + 2\frac{1}{L}\frac{\partial L}{\partial T}\right] = -\left[\xi + 2\lambda\right]\,, \tag{S6}$$

where L is the nanocrystal edge length. Since $\lambda \ll \xi$, the change of the slope of the effective band gap as function of temperature due to confinement is of the order of E_{qc}/E_g, which is always small, even for the smallest NCs.

$$\frac{\partial E_{qc}}{\partial T}\Big/\frac{\partial E_g}{\partial T} \sim -\frac{E_{qc}}{E_g}\,. \tag{S7}$$

Now we proceed to the g-factor value change with temperature. In the $\mathbf{k}\cdot\mathbf{p}$ method, its value is given by [29]

$$g_h(E_g, E_h) = 2 - \frac{4}{3}\frac{p^2 w_h}{m_0}\left[\frac{1}{E_g+E_h} - \frac{1}{E_g+E_h+\Delta}\right]\,, \tag{S8a}$$

$$g_e(E_g, E_e) = -\frac{2}{3} + \frac{4}{3}\frac{p^2}{m_0}\frac{w_e}{E_g+E_e} + \Delta g_{\mathrm{rem}} - 40\frac{m_0}{m_e}\frac{E_e}{\Delta}\,, \tag{S8b}$$

where $\Delta g_{\rm rem}$ is the correction from the remote bands and w_h, w_e account for the confinement-induced band mixing, see details in Ref. [29]. In equations above, in the electron g-factor we used a rough estimate for the term arising from the mixing with the spin-orbit split-off electron band, see Supporting Information of Ref. [29].

From Eq. (S8a) it follows that

$$\frac{\partial g_h}{\partial E_g} = \frac{\partial g_h}{\partial E_h} \tag{S9}$$

and the slope of the hole g-factor dependence on energy does not depend on the reason of the energy change, including the change as function of temperature.

For the electron g-factor the situation is more complicated. From Eq. (S8b) it follows that

$$\zeta_e^b \equiv \frac{\partial g_e}{\partial E_g} = -\frac{4}{3}\frac{p^2 w_e}{m_0}\frac{1}{(E_g+E_h)^2}\,, \tag{S10a}$$

$$\zeta_e^{qc} \equiv \frac{\partial g_e}{\partial E_e} = -\frac{4}{3}\frac{p^2 w_e}{m_0}\frac{1}{(E_g+E_h)^2} - 40\frac{m_0}{m_e}\frac{1}{\Delta}\,. \tag{S10b}$$

The second term in Eq. (S10b) is responsible for the deviation of the g-factors as function of quantum confinement energy in Fig. 2 of Ref. [29] from the universal dependence found in Ref. [27].

Next, we want to understand the evolution of the electron g-factor as function of the effective band gap when this change is due to a temperature change. The electron quantum confinement energy may be estimated as

$$E_e = \frac{\hbar^2}{2m_e}\frac{3\pi^2}{L^2} \tag{S11}$$

and

$$\frac{\partial E_e}{\partial T} = -E_e\left[\xi + 2\lambda\right]\,. \tag{S12}$$

Let us assume a small change of the temperature $\mathrm{d}T$, resulting in a change of the electron g-factor

$$\mathrm{d}g_e = \left[\frac{\partial g_e}{\partial E_g}\frac{\partial E_g}{\partial T} + \frac{\partial g_e}{\partial E_e}\frac{\partial E_e}{\partial T}\right]\mathrm{d}T\,, \tag{S13}$$

and the peak energy change

$$\mathrm{d}E(T) = \frac{\partial E_g}{\partial T}\mathrm{d}T + \frac{\partial E_{qc}}{\partial T}\mathrm{d}T\,. \tag{S14}$$

The value of interest for us is

$$\frac{\mathrm{d}g_e}{\mathrm{d}E(T)} \approx \zeta_e^b\left(1+\frac{E_{qc}}{E_g}\left(1+2\frac{\lambda}{\xi}\right)\right) - \zeta_e^{qc}\frac{E_e}{E_g}\left(1+2\frac{\lambda}{\xi}\right)\,, \tag{S15}$$

where we used $E_e,\ E_{qc} \ll E_g$.

Note that for $CsPbI_3$ NCs the "quantum confinement" contribution to the g-factor change relative to bulk is large: $\zeta_e^{qc} \sim -10$ eV^{-1}, while $\zeta_e^b \sim -2$ eV^{-1}. This means that the renormalization of the electron g-factor as a function of energy should be seen already when quantum confinement is small compared to the bulk band gap value. However, the change is expected to be small even for small nanocrystals and the bulk trend should be reproduced, in contrast to the experimental data.

To highlight the difference between the experimental data and the expected trend, we also analyze the change of the g-factor as function of the peak energy for different temperatures. For a particular sample, this value is perfectly fitted by a linear function from which $\frac{\partial g_e}{\partial E_g}$ may be extracted from the experimental data, see Fig. S7. As can be seen, this value changes from -9.2 eV^{-1} to -4.2 eV^{-1} when the temperature changes from 6 K to 120 K.

To check the theory expectations, we use the empirical tight-binding (ETB) method following Ref. [29]. To account for the temperature change, we adjust the parameter E_{pc} to reproduce the band gap change. We also change the lattice constant. The bulk values of the effective masses and g-factors change qualitatively following Eqs. (S5) and the results of Ref. [27] respectively. However, the value of the g-factor derivative with respect to E_g changes only marginally, see Fig. S7. The striking difference between theoretical analysis and experimental results show that an important ingredient is missing in the theoretical analysis.

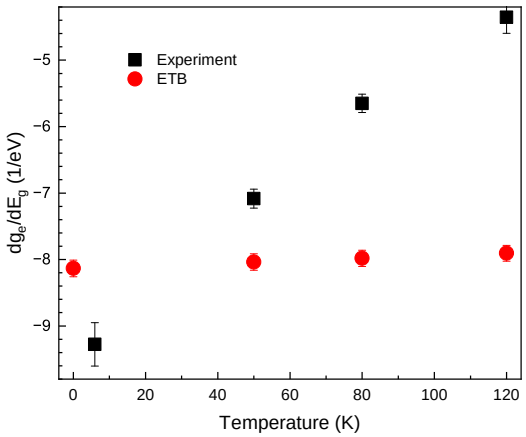

FIG. S7. Black squares show the experimentally measured $\frac{\partial g_e}{\partial E_g}$ for different temperatures. Red circles show the same value estimated from ETB calculations which take into account only the band gap change and the lattice extension. It is clear that the experimental trend is not reproduced in the atomistic calculations.